Optical constants of amorphous $SiO_2$ for photons in the range of 60-3000 eV



1999 J. Phys.: Condens. Matter 11 3355

(http://iopscience.iop.org/0953-8984/11/16/016)

J. Phys.: Condens. Matter **11** (1999) 3355–3370. Printed in the UK PII: S0953-8984(99)96248-3

# Optical constants of amorphous $SiO_2$ for photons in the range of 60–3000 eV

E Filatova†‡, V Lukyanov†, R Barchewitz‡§, J-M André‡§, M Idir‡‖ and Ph Stemmler‡‖

† Institute of Physics, St Petersburg University, St Petersburg 198904, Russia
‡ Laboratoire pour l'Utilisation du Rayonnement Electromagnetique (LURE), Université Paris Sud, 91898 Orsay cedex, France
§ Laboratoire de Chimie Physique, Université Pierre et Marie Curie, CNRS UMR 7416, 11 rue Pierre et Marie Curie, 75231 Paris cedex 05, France
‖ Commissariat à l'Energie Atomique, Centre de Bruyères-le-Châtel, BP12, 91680 Bruyères-le-Châtel, France

Received 27 July 1998, in final form 9 November 1998

**Abstract.** Optical constants of amorphous $SiO_2$ have been calculated by the Kramers–Kronig analysis in the continuous spectral region including Si $L_{2,3}$, O K and Si K absorption edges from the reflection spectra measured using synchrotron radiation. It is the first experiment carried out in such a wide energy region with the same sample. It has been found that for extrapolation of the experimental curve in the high energy region, where the photon energy exceeds the ionization potential of the Si K edge, the relation $R(E) \sim E^{-4}$ can be used for energies such that $\theta_c < \theta/2$ at small grazing angles.

## 1. Introduction

The most perfect data on optical constants are presented in [1, 3]. Nevertheless there are many gaps in optical constants of different materials especially in the soft-x-ray region near characteristic thresholds (in the regions of anomalous dispersion). The optical constants are traditionally calculated from angular dependencies of reflection by means of Fresnel formulas. In this case, optical constants at discrete photon energies are only obtained. In order to obtain the continuous spectral dependencies of optical constants, which is the most interesting around the absorption edges (high sensitivity to the phase composition and to the atomic arrangement of the reflector), a spectral dependency of reflection and a Kramers–Kronig analysis need to be applied. In general the application of the Kramers–Kronig integral may be accompanied by some difficulties. The central problem of such calculations is a limited energy region where the reflection coefficient can be measured and extrapolations have to be used outside the spectral range of the experiment.

In the paper we report on the dispersion of optical constants of amorphous $SiO_2$ in the 60–3000 eV photon energy range. We examine the problem of the calculation of the dispersion of optical data using Kramers–Kronig analysis more closely using the reflectance measurements carried out in a very wide energy range including Si $L_{2,3}$, O K and Si K absorption edges. It must be emphasized that we present the results of the first experiment carried out in such a wide energy region with the same sample and, besides, that the absolute values of the Si K reflection spectra are new too.

0953-8984/99/163355+16$19.50  

The purpose of the paper is also to assess the influence of the extrapolation outside the spectra range of the experiment in a high energy region on the accuracy of the values of optical constants, especially near the Si $L_{2,3}$ absorption edge.

## 2. Theoretical basis

### *2.1. Kramers–Kronig analysis*

Because of the low polarizibility of substances, the dielectric constant in the x-ray range can be conveniently represented in the form $\varepsilon = 1 - \varepsilon_1 + i\varepsilon_2 = (n + ik)^2$. Within the framework of the Fresnel model, the reflection amplitude of the s-polarized radiation can be written as:

$$r_s = \frac{\sin\theta - (\varepsilon - \cos^2\theta)^{1/2}}{\sin\theta + (\varepsilon - \cos^2\theta)^{1/2}} \tag{1}$$

where $\theta$ is the grazing angle. In the experiment, the reflection coefficient $R = |r|^2$ for intensities are measured. For the application of the Kramers–Kronig analysis one measures the reflectivity $R$ at a fixed grazing angle as a function of the photon energy. The complex reflection coefficient $r$ can be expressed in terms of its modulus $|r| = R^{1/2}$ and its phase shift appearing after reflection of the wave at the surface of the medium. By means of the Kramers–Kronig integral one can deduce the phase shift $\Psi(E_0)$:

$$\Psi(E_0) = \frac{E_0}{\pi} PV \int_0^\infty \frac{\ln R(E)}{E^2 - E_0^2}\,\mathrm{d}E. \tag{2}$$

Generally, the use of the Kramers–Kronig integral can involve difficulties, which are considered in [4–8]. Moreover since the integral (2) covers the whole energy range, the uncertainty in the determination of the phase shift is mainly caused by the limitation of the energy range covered by the reflectivity measurements. Outside the spectral range of the experiment, extrapolations of the reflection spectra have to be used.

### *2.2. Influence of the surface roughness on the reflection*

Most of the theories, e.g. Beckmann's simple scalar theory, are based on the condition that the mean roughness height $\sigma$ is less than the wavelength of the radiation $\lambda (\sigma \ll \lambda)$. The attenuation of the specular reflection, in this case, is generally given by the so-called Debye–Waller formula according to that the total integrated scattering only depends on the value of the rms roughness height $\sigma$. This theoretical condition is violated in the spectral range being considered.

In the strict sense, the total integrated scattering depends on both the value of the rms roughness height $\sigma$ and the radius of correlation $a$ [9–11]. According to [11] a smooth surface can be characterized by only fairly large radius of correlation $a$

$$a \gg \frac{\lambda}{\pi\theta_c^2}$$

$\theta_c$ being the critical angle. It should be emphasized that roughnesses with large radii of correlation do not contribute to radiation absorption and do not change the total radiation fluxes on the two sides of the interface. They only redistribute the intensity between the specular and scattered reflections. A distinction needs to be drawn between the total integrated scattering at small and large glancing angles. At the large glancing angles

$$\frac{\pi a\theta^2}{\lambda} \gg 1 \qquad \frac{\pi a\theta_c^2}{\lambda} \gg 1$$

the total integrated scattering depends only on the value of the rms roughness height $\sigma$ whereas it depends on the rms roughness height $\sigma$ as well as the radius of correlation $a$ at the small glancing angles [12]

$$\frac{\pi a\theta^2}{\lambda} \ll 1 \qquad \frac{\pi a\theta_c^2}{\lambda} \gg 1.$$

From the above reasoning the attenuation of the specular reflection can be written as follows [12]:

$$R = R_F \exp\left[-\left(\frac{4\pi}{\lambda}\sigma \sin\theta\right)^2\right] \qquad \text{at large glancing angle } \theta \tag{3a}$$

$$R = R_F \exp\left[-\left(\frac{2\pi}{\lambda}\right)^{3/2} \frac{\sigma^2}{\sqrt{a}}\theta\right] \qquad \text{at small glancing angle } \theta \tag{3b}$$

where $R$ is the reflectivity of a rough surface, $R_F$ is the reflectivity of a perfect surface, $\sigma$ is rms height, $a$ is radius of correlation.

## 3. Experimental procedure and sample

The angular and spectral dependencies of reflectivity near the Si K absorption edge were carried out in a reflectometer set-up on the SB3 synchrotron beamline 'MOGOTOX' (monochromator and goniometer for x-ray optics treatment) of the Super-ACO storage ring of LURE at Orsay. Figure 1 presents the MOGOTOX device; it is composed of two chambers located at 11 and 13 m from the source respectively. The first one contains the entrance slit and is used as a vacuum buffer between the ring and the second measurement chamber. The second chamber contains a filter holder, an energy low-pass filter, a double-crystal monochromator, a $\theta$–$2\theta$ goniometer and a detector. The first crystal of the monochromator has rotational and translational adjustments whereas the second one has only rotational adjustment. The crystal rotation can be varied from 5 to 85 degrees. This allows us to cover the energy range from 0.8 to 8 keV, using different crystal pairs. (111) InSb crystal sheets, the reflectivity of which is close to 60%, were used in the experiment. The energy resolution near Si K was better than

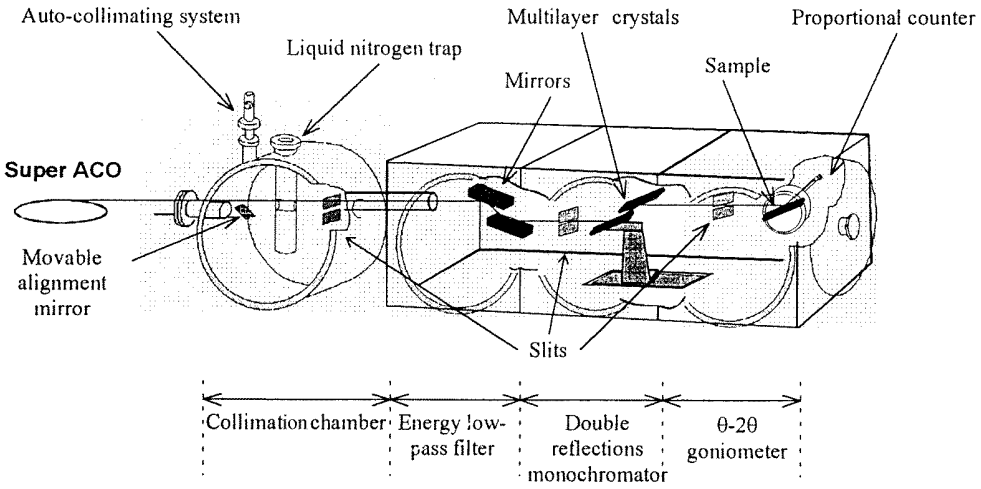


**Figure 1.** MOGOTOX device: experimental set-up for x-ray optics and detector calibration.

0.8 eV. The $\theta$–$2\theta$ goniometer has several degrees of freedom that permit us to locate the sample relative to the incident beam. The detector is a gas flow proportional counter closed with a system composed with a polypropylene window supported by a metallic grid. It works with a 90%/10% argon/methane mixture. High spectral purity was achieved by using the detector in the proportionality mode with a single channel analyser.

A sample with an $SiO_2$ layer of 120 nm thickness on a top of an Si substrate was investigated. The Si substrate is a 0.8 mm thick disc of (111) single-crystal silicon of p type; the diameter of the disc is 7.6 cm. The value of rms roughness is smaller than 1 nm. The sample was prepared by a dry oxidation method at about 1050 °C. In this case the surface of the sample is formed in the process of spontaneous growth of dioxide on the crystalline silicon plate.

## 4. Results and discussion

### *4.1. Reflection spectra*

Figure 2 shows the Si K reflection spectra $R(E)$ obtained for different glancing angles ($\theta = 0.6^\circ$, $0.8^\circ$, $1^\circ$). These spectra are similar in shape to the reflection spectra obtained in [13]. It should be stressed that spectra measured in [13] were obtained in arbitrary units.

Due to the limited size of the sample and the size of the beam, the reflected radiation is only partially detected at more grazing angles. As can be seen in figure 2, the spectra are similar in number of features and in their energy positions. The maxima a and b in the spectrum at $1^\circ$ are caused purely by interference.

The reflection spectrum at the grazing angle of $0.6^\circ$ measured in the wide energy range 1800–3000 eV was chosen to calculate the optical constants. In this case, the $SiO_2$ layer is thick enough for radiation almost not to penetrate through it. This spectrum was joined with the data obtained for the same sample in the soft-x-ray region (50–900 eV) [14, 15].

Recall that the atoms in condensed systems can be considered as independent scattering dipoles (the effect of electron charge redistribution in solids on the tensor of atomic scattering factor in the normal dispersion region is small enough to be neglected) in the range of normal

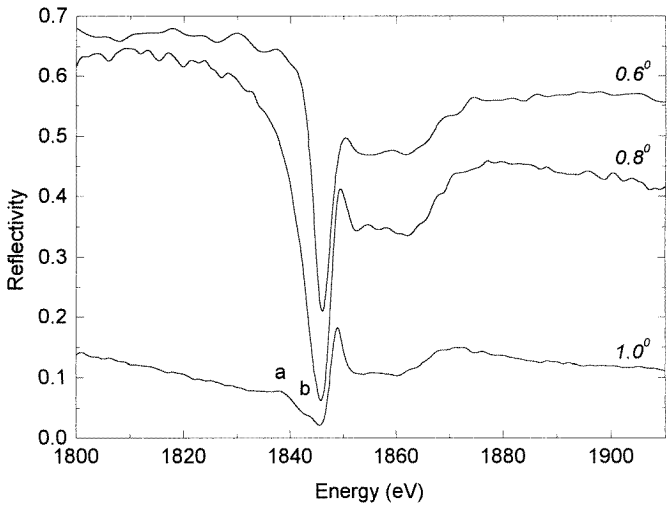


**Figure 2.** Si K reflection spectra of $SiO_2$ for grazing angles $\theta = 0.6^\circ$, $0.8^\circ$, $1^\circ$.

**Table 1.** Optical constants for amorphous $SiO_2$ prepared by a dry oxidation method at ∼1050 °C (mass density $\rho$ was 2.3 g cm$^{-3}$) calculated from spectral dependency of reflection using Kramers–Kronig analysis. Data calculated from angular dependencies of reflection [14] are given in brackets.

| eV | Å | $n$ | $k$ |
|---|---|---|---|
| 65.0 | 190.73 | 0.957 93 | $2.727 \times 10^{-2}$ |
| 69.0 | 179.68 | 0.959 61 | 2.405 |
| 73.0 | 169.83 | 0.962 37 | 2.097 |
| 77.0 | 161.01 | 0.965 66 | 1.848 |
| 81.0 | 153.06 | 0.968 20 | 1.664 |
| 84.5 | 146.72 | 0.970 44 | 1.509 |
| 87.1 | 142.34 | 0.971 86 | 1.403 |
| 90.0 | 137.75 | 0.973 85 | 1.269 |
| 92.5 | 134.03 | 0.975 12 | 1.167 |
| 95.0 | 130.50 | 0.976 65 | $1.076 \times 10^{-2}$ |
| 98.0 | 126.51 | 0.978 79 | $9.574 \times 10^{-3}$ |
| 99.5 | 124.60 | 0.979 85 | 9.143 |
| 100.0 | 123.98 | 0.980 26 | 9.006 |
| 103.0 | 120.36 | 0.983 11 | 8.257 |
| 104.3 | 118.86 | 0.985 06 | 7.927 |
| 104.4 | 118.75 | 0.985 24 | 7.881 |
| 104.5 | 118.64 | 0.985 50 | 7.841 |
| 104.6 | 118.52 | 0.985 80 | 7.813 |
| 104.7 | 118.41 | 0.986 13 | 7.879 |
| 104.8 | 118.30 | 0.986 38 | 7.865 |
| 104.9 | 118.18 | 0.986 76 | 7.830 |
| 105.0 | 118.07 | 0.987 24 | 7.902 |
| 105.1 | 117.96 | 0.987 69 | 8.071 |
| 105.2 | 117.85 | 0.988 18 | 8.311 |
| 105.4 | 117.62 | 0.989 21 | $9.158 \times 10^{-3}$ |
| 105.5 | 117.51 | 0.989 60 | $1.001 \times 10^{-2}$ |
| 105.6 | 117.40 | 0.989 68 | 1.091 |
| 105.7 | 117.29 | 0.989 53 | 1.180 |
| 105.9 | 117.07 | 0.988 38 | 1.288 |
| 106.0 | 116.96 | 0.987 74 | 1.291 |
| 106.1 | 116.85 | 0.987 35 | 1.276 |
| 106.2 | 116.74 | 0.987 20 | 1.258 |
| 106.3 | 116.63 | 0.987 16 | 1.250 |
| 106.4 | 116.52 | 0.987 11 | 1.251 |
| 106.5 | 116.41 | 0.986 98 | 1.244 |
| 106.6 | 116.30 | 0.986 93 | 1.224 |
| 106.7 | 116.19 | 0.987 09 | 1.190 |
| 106.8 | 116.08 | 0.987 51 | 1.171 |
| 106.9 | 115.97 | 0.988 06 | 1.176 |
| 107.0 | 115.87 | 0.988 57 | 1.197 |
| 107.1 | 115.76 | 0.989 13 | 1.239 |
| 107.4 | 115.43 | 0.989 92 | 1.446 |
| 107.5 | 115.33 | 0.989 87 | 1.532 |
| 107.9 | 114.90 | 0.988 03 | 1.843 |
| 108.0 | 114.79 | 0.987 13 | 1.914 |
| 108.1 | 114.69 | 0.986 04 | 1.945 |
| 108.2 | 114.58 | 0.985 17 | 1.961 |
| 108.3 | 114.47 | 0.984 18 | 1.964 |
| 108.4 | 114.37 | 0.983 23 | 1.942 |
| 108.5 | 114.26 | 0.982 38 | 1.925 |
| 108.9 | 113.84 | 0.979 57 | 1.683 |

**Table 1.** (Continued)

| eV | Å | *n* | *k* |
|---|---|---|---|
| 109.0 | 113.74 | 0.979 26 | 1.613 |
| 109.1 | 113.63 | 0.979 05 | 1.526 |
| 109.2 | 113.53 | 0.979 07 | 1.448 |
| 109.3 | 113.43 | 0.979 16 | 1.384 |
| 110.1 | 112.60 | 0.981 31 | 1.060 |
| 110.2 | 112.50 | 0.981 67 | 1.048 |
| 110.3 | 112.40 | 0.981 95 | 1.046 |
| 110.4 | 112.30 | 0.982 17 | 1.041 |
| 110.5 | 112.20 | 0.982 43 | 1.036 |
| 110.6 | 112.09 | 0.982 66 | 1.041 |
| 110.7 | 111.99 | 0.982 79 | 1.038 |
| 110.8 | 111.89 | 0.983 01 | 1.038 |
| 111.1 | 111.59 | 0.983 45 | 1.047 |
| 111.2 | 111.49 | 0.983 58 | 1.046 |
| 111.6 | 111.09 | 0.983 94 | 1.068 |
| 112.5 | 110.20 | 0.984 52 | 1.071 |
| 113.4 | 109.33 | 0.985 20 | 1.113 |
| 116.5 | 106.42 | 0.983 88 | $1.126 \times 10^{-2}$ |
| 119.7 | 103.57 | 0.985 94 | $9.207 \times 10^{-3}$ |
| 122.9 | 100.88 | 0.988 13 | $1.028 \times 10^{-2}$ |
| 126.2 | 98.24 | 0.988 11 | 1.196 |
| 129.6 | 95.66 | 0.987 07 | 1.249 |
| 133.1 | 93.14 | 0.986 09 | 1.185 |
| 136.7 | 90.69 | 0.985 64 | $1.070 \times 10^{-2}$ |
| 140.4 | 88.30 | 0.985 75 | $9.498 \times 10^{-3}$ |
| 144.2 | 85.97 | 0.986 37 | 8.448 |
| 148.1 | 83.71 | 0.987 06 | 7.671 |
| 152.2 | 81.46 | 0.988 05 | 7.183 |
| 156.3 | 79.32 | 0.988 86 | 7.091 |
| 160.5 | 77.24 | 0.988 08 | 7.003 |
| 164.8 | 75.23 | 0.988 87 | 6.306 |
| 169.3 | 73.23 | 0.989 36 | 5.898 |
| 173.9 | 71.29 | 0.989 82 | 5.558 |
| 178.6 | 69.41 | 0.990 14 | 5.165 |
| 183.5 | 67.56 | 0.990 61 | 4.840 |
| 188.5 | 65.77 | 0.991 04 | 4.607 |
| 193.5 | 64.07 | 0.991 33 | 4.430 |
| 199.0 | 62.30 | 0.991 54 | 4.171 |
| 204.0 | 60.77 | 0.991 81 | 3.883 |
| 209.5 | 59.18 | 0.992 09 | 3.592 |
| 215.5 | 57.53 | 0.992 38 | 3.280 |
| 221.0 | 56.10 | 0.992 68 | 2.985 |
| 227.0 | 54.61 | 0.993 01 | 2.714 |
| 233.0 | 53.21 | 0.993 34 | 2.481 |
| 239.5 | 51.76 | 0.993 68 | 2.257 |
| 246.0 | 50.40 | 0.993 99 | 2.068 |
| 252.5 | 49.10 | 0.994 31 | 1.873 |
| 259.5 | 47.77 | 0.994 64 | 1.715 |
| 266.5 | 46.52 | 0.994 96 | 1.625 |
| 273.5 | 45.33 | 0.995 23 | 1.504 |
| 450.0 | 27.55 | [0.998 17] | [3.535] |
| 500.0 | 24.80 | [0.998 65] | [2.545] |
| 510.0 | 24.31 | [0.998 75] | [2.405] |

**Table 1.** (Continued)

| eV | Å | $n$ | $k$ |
|---|---|---|---|
| 520.0 | 23.84 | [0.998 88] | [2.315] |
| 524.7 | 23.63 | 0.998 94 | 2.457 |
| 527.7 | 23.49 | 0.999 01 | 2.492 |
| 529.7 | 23.40 | 0.999 08 | 2.533 |
| 531.2 | 23.34 | 0.999 16 | 2.859 |
| 531.7 | 23.32 | 0.999 18 | 3.033 |
| 532.2 | 23.29 | 0.999 19 | 3.229 |
| 532.7 | 23.27 | 0.999 23 | 3.100 |
| 533.2 | 23.25 | 0.999 29 | 3.322 |
| 533.7 | 23.23 | 0.999 31 | 3.660 |
| 534.7 | 23.19 | 0.999 39 | 4.230 |
| 535.2 | 23.16 | 0.999 42 | 4.662 |
| 535.7 | 23.14 | 0.999 46 | 5.659 |
| 536.2 | 23.12 | 0.999 46 | 6.741 |
| 536.7 | 23.10 | 0.999 46 | 7.695 |
| 537.2 | 23.08 | 0.999 42 | $8.772 \times 10^{-4}$ |
| 538.2 | 23.04 | 0.999 23 | $1.031 \times 10^{-3}$ |
| 538.7 | 23.01 | 0.999 12 | 1.040 |
| 539.2 | 22.99 | 0.999 03 | $1.023 \times 10^{-3}$ |
| 539.7 | 22.97 | 0.998 93 | $9.732 \times 10^{-4}$ |
| 540.2 | 22.95 | 0.998 91 | 9.703 |
| 540.7 | 22.93 | 0.998 84 | 9.439 |
| 541.2 | 22.91 | 0.998 80 | 8.431 |
| 541.7 | 22.89 | 0.998 81 | 8.337 |
| 542.2 | 22.87 | 0.998 79 | 8.267 |
| 542.7 | 22.84 | 0.998 75 | 7.960 |
| 544.2 | 22.78 | 0.998 74 | 7.130 |
| 546.2 | 22.70 | 0.998 74 | 6.345 |
| 548.2 | 22.61 | 0.998 78 | 5.644 |
| 549.2 | 22.57 | 0.998 79 | 5.476 |
| 550.7 | 22.51 | 0.998 83 | 5.299 |
| 565.7 | 21.92 | 0.998 77 | 6.376 |
| 580.7 | 21.35 | 0.998 80 | 4.791 |
| 595.7 | 20.81 | 0.998 86 | 4.373 |
| 610.7 | 20.30 | 0.998 90 | 4.336 |
| 620.7 | 19.97 | 0.998 90 | 4.118 |
| 630.7 | 19.66 | 0.998 92 | 3.845 |
| 640.7 | 19.35 | 0.998 94 | 3.618 |
| 655.5 | 18.91 | 0.998 98 | 3.271 |
| 670.5 | 18.49 | 0.999 02 | 2.983 |
| 685.5 | 18.09 | 0.999 05 | 2.724 |
| 700.0 | 17.71 | 0.999 09 | 2.545 |
| 715.0 | 17.34 | 0.999 12 | 2.401 |
| 730.0 | 16.98 | 0.999 15 | 2.265 |
| 745.0 | 16.64 | 0.999 18 | 2.113 |
| 760.0 | 16.31 | 0.999 21 | 1.966 |
| 775.0 | 16.00 | 0.999 24 | 1.827 |
| 790.0 | 15.69 | 0.999 26 | 1.699 |
| 805.0 | 15.40 | 0.999 29 | 1.592 |
| 820.0 | 15.12 | 0.999 31 | 1.491 |
| 835.0 | 14.85 | 0.999 32 | 1.356 |
| 850.0 | 14.59 | 0.999 37 | 1.220 |
| 865.0 | 14.33 | 0.999 38 | 1.132 |
| 880.0 | 14.09 | 0.999 40 | 1.113 |

**Table 1.** (Continued)

| eV | Å | $n$ | $k$ |
|---|---|---|---|
| 895.0 | 13.85 | 0.999 42 | $1.048 \times 10^{-4}$ |
| 910.0 | 13.62 | 0.999 44 | $9.946 \times 10^{-5}$ |
| 925.0 | 13.40 | 0.999 46 | 9.593 |
| 940.1 | 13.19 | 0.999 47 | 9.062 |
| 955.1 | 12.98 | 0.999 49 | 8.539 |
| 970.1 | 12.78 | 0.999 51 | 8.101 |
| 985.1 | 12.59 | 0.999 52 | 7.687 |
| 1000.1 | 12.40 | 0.999 53 | 7.294 |
| 1050.1 | 11.81 | 0.999 58 | 6.180 |
| 1100.1 | 11.27 | 0.999 61 | 5.246 |
| 1150.1 | 10.78 | 0.999 65 | 4.485 |
| 1200.1 | 10.33 | 0.999 68 | 3.863 |
| 1250.1 | 9.92 | 0.999 70 | 3.348 |
| 1300.1 | 9.54 | 0.999 73 | 2.915 |
| 1355.1 | 9.15 | 0.999 75 | 2.520 |
| 1405.1 | 8.82 | 0.999 77 | 2.221 |
| 1455.1 | 8.52 | 0.999 78 | 1.966 |
| 1500.1 | 8.26 | 0.999 80 | 1.766 |
| 1550.1 | 8.00 | 0.999 81 | 1.574 |
| 1600.1 | 7.75 | 0.999 82 | 1.406 |
| 1645.1 | 7.54 | 0.999 83 | 1.273 |
| 1700.1 | 7.29 | 0.999 85 | $1.128 \times 10^{-5}$ |
| 1750.1 | 7.08 | 0.999 86 | $9.898 \times 10^{-6}$ |
| 1795.1 | 6.91 | 0.999 87 | 8.911 |
| 1840.1 | 6.738 | 0.999 90 | 8.990 |
| 1842.6 | 6.728 | 0.999 91 | 8.784 |
| 1842.7 | 6.728 | 0.999 91 | 8.802 |
| 1842.8 | 6.728 | 0.999 91 | 8.851 |
| 1842.9 | 6.727 | 0.999 91 | 8.934 |
| 1843.4 | 6.726 | 0.999 92 | $9.955 \times 10^{-6}$ |
| 1844.6 | 6.721 | 0.999 93 | $1.822 \times 10^{-5}$ |
| 1845.8 | 6.717 | 0.999 95 | 4.418 |
| 1846.0 | 6.716 | 0.999 96 | 5.481 |
| 1846.1 | 6.716 | 0.999 96 | 6.145 |
| 1846.2 | 6.715 | 0.999 96 | 6.889 |
| 1846.3 | 6.715 | 0.999 96 | 7.708 |
| 1846.4 | 6.715 | 0.999 96 | 8.579 |
| 1846.5 | 6.714 | 0.999 95 | $9.470 \times 10^{-5}$ |
| 1847.0 | 6.712 | 0.999 91 | $1.276 \times 10^{-4}$ |
| 1847.1 | 6.712 | 0.999 90 | 1.289 |
| 1847.2 | 6.712 | 0.999 89 | 1.280 |
| 1847.3 | 6.711 | 0.999 88 | 1.251 |
| 1847.4 | 6.711 | 0.999 87 | $1.203 \times 10^{-4}$ |
| 1847.7 | 6.710 | 0.999 85 | $9.930 \times 10^{-5}$ |
| 1847.8 | 6.710 | 0.999 84 | 9.148 |
| 1847.9 | 6.709 | 0.999 84 | 8.385 |
| 1848.0 | 6.709 | 0.999 84 | 7.669 |
| 1848.1 | 6.708 | 0.999 84 | 7.017 |
| 1848.2 | 6.708 | 0.999 84 | 6.435 |
| 1848.3 | 6.708 | 0.999 84 | 5.922 |
| 1848.9 | 6.706 | 0.999 85 | 3.986 |
| 1849.9 | 6.702 | 0.999 87 | 3.102 |
| 1850.0 | 6.702 | 0.999 87 | 3.085 |

**Table 1.** (Continued)

| eV | Å | $n$ | $k$ |
|---|---|---|---|
| 1850.1 | 6.701 | 0.999 87 | 3.073 |
| 1850.2 | 6.701 | 0.999 87 | 3.067 |
| 1850.3 | 6.700 | 0.999 87 | 3.066 |
| 1850.4 | 6.700 | 0.999 87 | 3.068 |
| 1850.5 | 6.700 | 0.999 87 | 3.074 |
| 1851.6 | 6.696 | 0.999 88 | 3.289 |
| 1852.7 | 6.692 | 0.999 88 | 3.489 |
| 1853.6 | 6.689 | 0.999 88 | 3.509 |
| 1855.0 | 6.683 | 0.999 88 | 3.507 |
| 1900.2 | 6.525 | 0.999 88 | 1.975 |
| 1950.2 | 6.357 | 0.999 88 | 2.097 |
| 2000.2 | 6.198 | 0.999 89 | 1.928 |
| 2045.2 | 6.062 | 0.999 89 | 1.781 |
| 2095.2 | 5.917 | 0.999 89 | 1.634 |
| 2140.2 | 5.793 | 0.999 90 | 1.514 |
| 2190.2 | 5.661 | 0.999 90 | 1.394 |
| 2240.2 | 5.534 | 0.999 91 | 1.285 |
| 2285.2 | 5.425 | 0.999 91 | 1.196 |
| 2320.2 | 5.343 | 0.999 91 | 1.132 |
| 2370.2 | 5.231 | 0.999 91 | $1.048 \times 10^{-5}$ |
| 2410.3 | 5.144 | 0.999 92 | $9.859 \times 10^{-6}$ |
| 2460.3 | 5.039 | 0.999 92 | 9.149 |
| 2500.3 | 4.959 | 0.999 92 | 8.627 |
| 2550.3 | 4.861 | 0.999 93 | 8.025 |
| 2600.3 | 4.768 | 0.999 93 | 7.476 |
| 2655.3 | 4.669 | 0.999 93 | 6.923 |
| 2705.3 | 4.583 | 0.999 93 | 6.460 |
| 2755.3 | 4.500 | 0.999 94 | 6.059 |
| 2805.3 | 4.420 | 0.999 94 | 5.672 |
| 2850.3 | 4.350 | 0.999 94 | 5.354 |
| 2900.3 | 4.275 | 0.999 94 | 5.019 |
| 2945.3 | 4.209 | 0.999 94 | 4.750 |
| 2980.3 | 4.160 | 0.999 95 | 4.563 |
| 3000.3 | 4.132 | 0.999 95 | 4.462 |

dispersion where the photon energy is far from the absorption edges. Then, the total atomic dipole moment is proportional to the average atomic factor of the medium. With this result we can use the data of the atomic scattering factor from the table of Henke [1] in the ranges of normal dispersion, specifically in the range 900–1800 eV aligned far from O K and Si K absorption edges.

The data were connected as follows. Using refined optical constants derived from the experimental spectrum measured at the grazing angle of $2^\circ$ in the energy range 50–900 eV, the reflection spectrum at $0.6^\circ$ was calculated. Unfortunately this operation is inevitable and is motivated by the special features of the experimental conditions in the soft-x-ray range. The calculated spectrum and the spectrum measured at $0.6^\circ$ in the energy range 1800–3000 eV (figure 2) corrected for the surface roughness by equation (3*b*) were compared with the reflection coefficients calculated from the atomic scattering factor [1] in the regions of normal dispersion. For the smooth combination of the data, a fitting analysis varying the ratio $\sigma^2/\sqrt{a}$ was used. The value of mass density was fixed and equal to 2.3 g cm$^{-3}$ derived in [14] and [15].

Figure 3 shows the reflection spectrum at $\theta = 0.6^\circ$ in a wide energy region, including

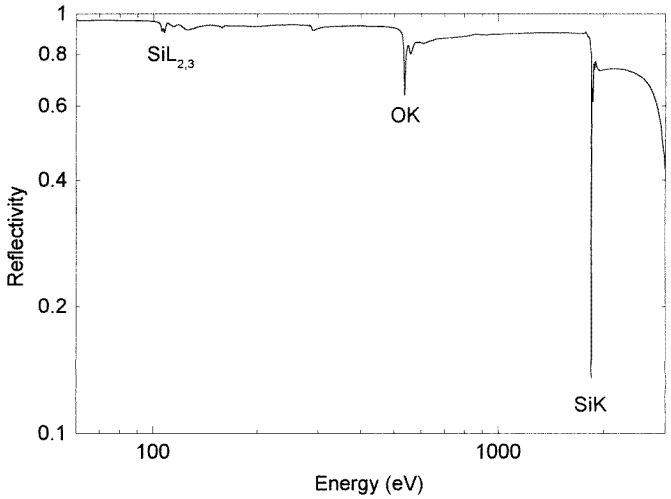


**Figure 3.** Reflection spectrum at $\theta = 0.6^\circ$ in a wide energy region, including Si $L_{2,3}$, O K and Si K absorption edges corrected for the surface roughness.

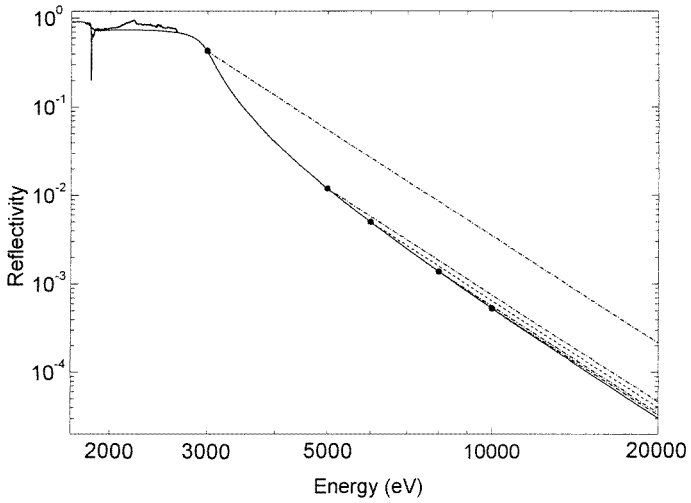


**Figure 4.** Spectral dependency of the reflection coefficient at $\theta = 0.6^\circ$ in the energy region from 1.8 keV to 20 keV. The bold-faced curve denotes the experimental curve, the full curve the data based on the results of [1]; the dashed curves denote the extrapolation by the relation $R(E) \sim E^{-4}$ from different separate energies indicated by circles.

Si $L_{2,3}$, O K and Si K absorption edges corrected for the surface roughness.

Analysis of angular dependencies of the reflection measured at discrete points in the spectral range 50–3000 eV have provided control of the normalization of the reflection coefficients obtained. The extrapolation of $R(\theta)$ to the point $\theta = 0$ should exactly give $R = 1$. Although this point is experimentally inaccessible, the approximation performed allows one to examine the normalization of the experimental curves.

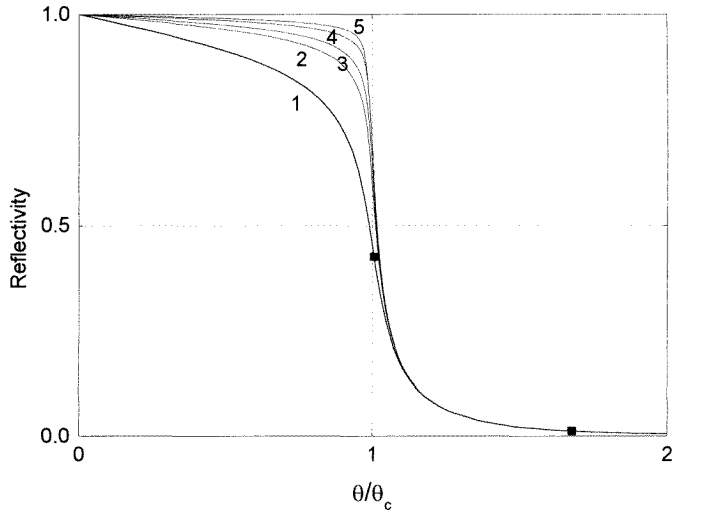


(a)

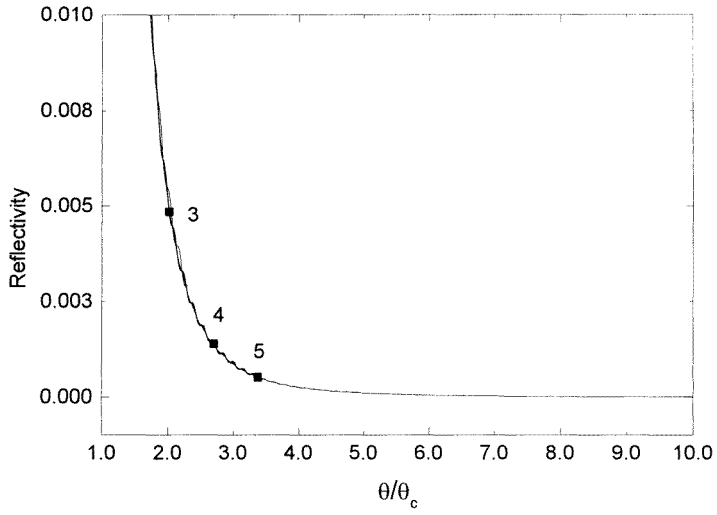


(b)

**Figure 5.** (a) Angular dependencies of the reflection coefficient at separated energies: 1, 3 keV; 2, 5 keV; 3, 6 keV; 4, 8 keV; 5, 10 keV. Squares identify the position of grazing $\theta = 0.6^\circ$ in the angular curves. (b) A magnification of the region of small reflection coefficient values.

### *4.2. Dispersion of the optical constants*

As pointed out above, to give the optical constants by means of the Kramers–Kronig relation, extrapolation outside the experimental range is called for. In order to obtain a smooth connection of the experimental spectra with the extrapolation curve, one can use, according to our earlier investigation [14, 15] in the low energy range, the following extrapolation,

$$R(E) = R(E_1) + (1 - R(E_1))\left(1 - \frac{E}{E_1}\right)^{1/2} \tag{4}$$

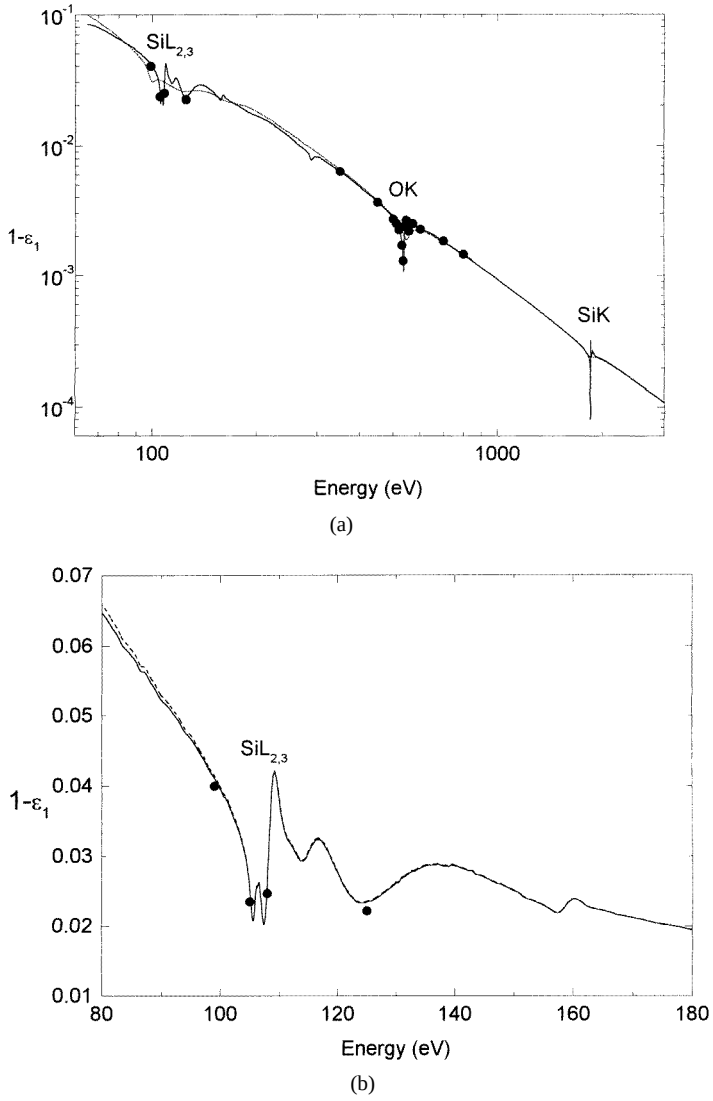


**Figure 6.** (a) Spectral dependency of the real part $1-\varepsilon_1$ of the dielectric constant. The solid curve is the calculation from the reflection spectrum for a grazing angle $\theta = 0.6^\circ$; the dotted curve is the calculated based on the results of [1]; circles are the data obtained from the angular dependent measurements [14]. (b) A magnification of the region around the Si $L_{2,3}$ edge. (c) A magnification of the region around the O K edge. (d) A magnification of the region around the Si K edge. The dashed curve is the calculation from the reflection spectrum measured in the range 50–900 eV at the grazing angle $2^\circ$.

from the point $E_1$ = 50 eV to $R = 1$ at $E = 0$. In the high energy region, where the photon energy exceeds the ionization potential of the Si K edge, the law of absorption $\mu(E) \sim E^{-3}$ is valid. Using Fresnel formulas and the fact that in the region of normal dispersion $\delta/\lambda^2 = \text{const}$ (where $n + \mathrm{i}k = 1 - \delta + \mathrm{i}k$) the relation $R(E) \sim E^{-4}$ can be obtained. By this means, the spectrum was extrapolated according to the relation $R(E) \sim E^{-4}$ from the point $E_2 = 3000$ eV.

In the context of the preceeding, the dispersion of optical constants was derived. The optical constants obtained at discrete energy points by means of analysis of angular dependencies

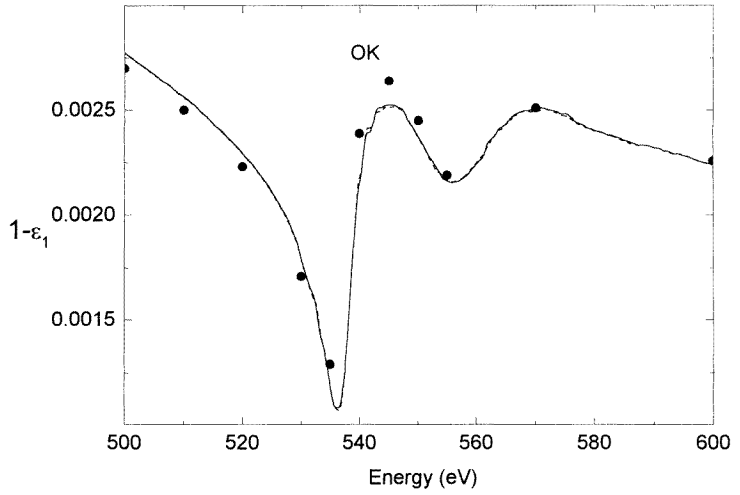


(c)

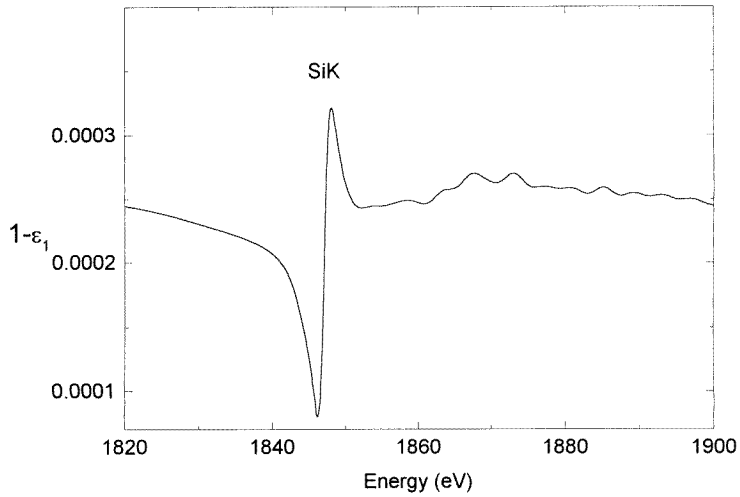


(d)

**Figure 6.** (Continued)

of the reflection coefficient from [14] were used to control over the optical constants calculated by the Kramers–Kronig integral. The data calculated in the frame of the above-mentioned extrapolation was found to be larger by about 80% as compared to controlled data.

In order to appreciate the cause of such huge discrepancies, let us call attention to the angular and spectral dependencies of the reflection coefficient at the energies larger than 3 keV. Because this energy range is aligned in the range of normal dispersion (far from absorption edges), the values of atomic factor from [1] are useful in the calculation of the reflection coefficients. Figure 4 shows the spectral dependency of the reflection coefficient at the grazing angle of $0.6^\circ$ in the energy region from 1.8 keV to 20 keV (there is the experimental curve in the region 1.8 keV to 2.7 keV and there are the data based on the results of [1] for energies larger than 2.7 keV). The extrapolation from the relation $R(E) \sim E^{-4}$ from different separated

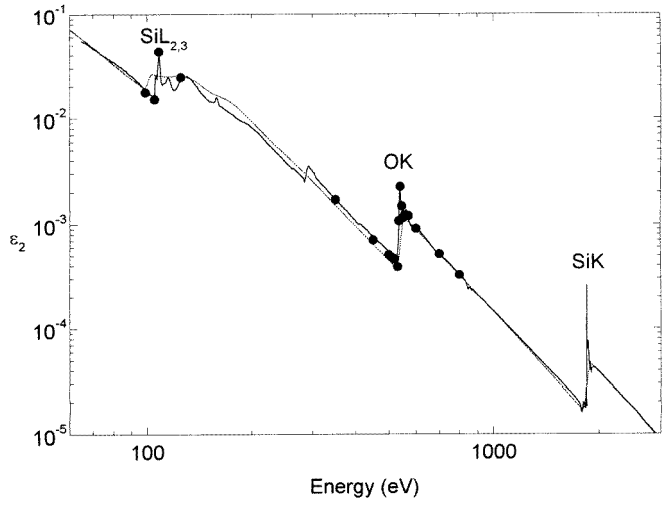


(a)

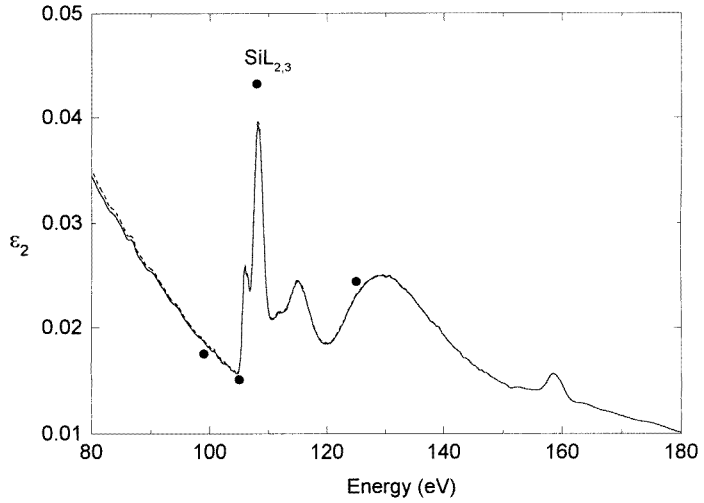


(b)

**Figure 7.** (a) Spectral dependency of the imaginary part $\varepsilon_2$ of the dielectric constant. The solid curve is the calculation from the reflection spectrum for a grazing angle $\theta = 0.6^\circ$; the dotted curve is the calculation based on the results of [1]; circles are the data obtained from the angular dependent measurements [14]. (b) A magnification of the region around the Si $L_{2,3}$ edge. (c) A magnification of the region around the O K edge. (d) A magnification of the region around the Si K edge. The dashed curve is the calculation from the reflection spectrum measured in the range 50–900 eV for a grazing angle $\theta = 2^\circ$.

energies is presented too. As will be seen from figure 4, the relation $R(E) \sim E^{-4}$ breaks down for energies where the reflection coefficient varies only slightly (in the total external reflection region). The behaviour of the reflection coefficient is reasonably described by this relation only at high energies larger than around 8 keV.

Figure 5 shows the angular dependencies of the reflection coefficient at separated energies (these energies are marked on figure 4 by circles). Squares identify the position of the grazing

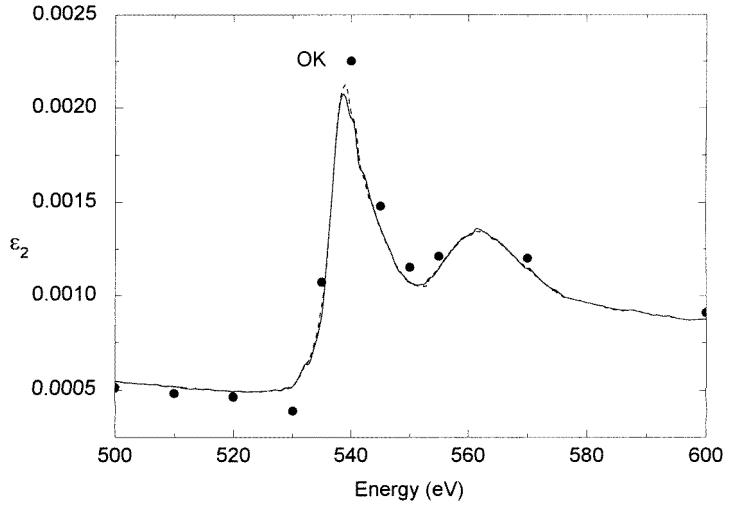


(c)

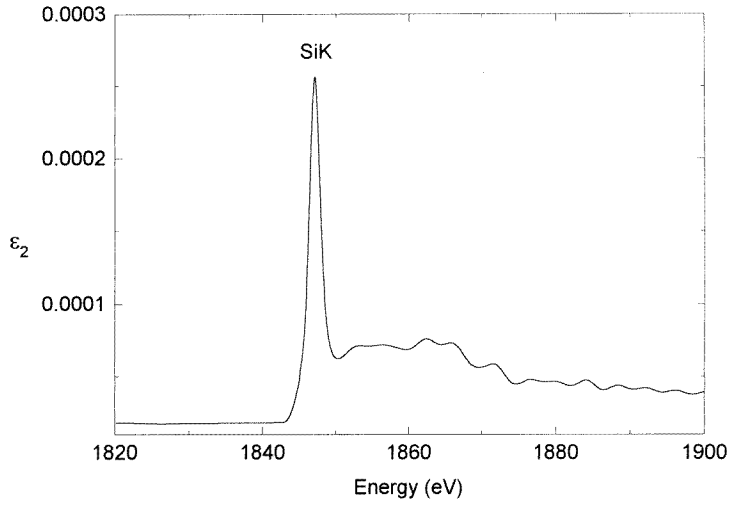


(d)

**Figure 7.** (Continued)

angle $0.6^\circ$ in the angular curves. One can easily see that there are three extreme cases in the angular dependency of the reflection coefficient $R(\theta)$. In the first region, the reflection coefficient is great and varies only slightly (the total external reflection region). The second one is the region where the reflectivity decreases drastically. In the third region, the reflection is negligibly small for all energies. From figure 5, we notice that the reflection coefficient at the grazing angle $0.6^\circ$ is brought into the third region for all energies larger than 8 keV. Because, for the energy 8 keV, the ratio $\theta/\theta_c$ is about 2.5 at $\theta = 0.6^\circ$, one is inclined to think that the relation $R(E) \sim E^{-4}$ holds for energies such that $\theta_c < \theta/2$.

The dispersion of optical constants was derived using extrapolation from different energy points from the relation $R(E) \sim E^{-4}$ to consider the influence of the extrapolation on the value of optical constants.

It was found that the greatest relative error occurs when the extrapolation is carried out from the energy such that $\theta = 0.6^\circ$ is in the second range (figure 5) and was in excess of 50%. Extrapolation carried out from energies larger than 8 keV gives practically the same values of optical constants.

Figures 6 and 7 show the calculated spectral dependencies of real $(1-\varepsilon_1)$ and imaginary $\varepsilon_2$ parts of the dielectric constant $\varepsilon$ in the region 50–3000 eV using extrapolation carried out from 8 keV. Table 1 lists the calculated optical constants. We have elected to tabulate $n$ and $k$ because it is then an easy matter to obtain $1 - \varepsilon_1 = n^2 - k^2$ and $\varepsilon_2 = 2nk$ as well as reflectivity $R$.

From figures 6 and 7, we notice that a consideration of the Si K absorption edge does not affect the values of optical data near Si $L_{2,3}$ and O K absorption edges. Brief mention should be made of a peak at about 300 eV. Analysis of the calculated spectra as well as reflection spectra allows us to connect this structure with carbon. Analysis of the calculated optical data in the region 300–550 eV points to the fact the values derived from spectral dependencies of reflection using Kramers–Kronig analysis are higher than those predicted from data based on the results of [1] and from angular dependencies of reflection in this energy region.

## 5. Conclusions

In this paper, the optical constants of amorphous $SiO_2$ have been calculated by the Kramers–Kronig analysis in the continuous spectral region including Si $L_{2,3}$, O K and Si K absorption edges from the reflection spectra measured using synchrotron radiation. It has been found that a consideration of the Si K absorption edge does not affect the values of optical data near Si $L_{2,3}$ and O K absorption edges.

It was demonstrated that for the extrapolation of the experimental curve in the high energy region, where the photon energy exceeds the ionization potential of the Si K edge, the relation $R(E) \sim E^{-4}$ can be used for energies such that $\theta_c < \theta/2$ at small angles. It may be assumed that this criterion is valid for large angles. According to this criterion, the point of the beginning of extrapolation will move in the direction of decreasing energy as the grazing angle increases. With the growth of the angle $\theta$, the energy region needed to measure the reflection spectrum will be narrowed.

## References


[1] Henke B L, Gullikson E M and Davis J C 1993 *At. Data Nucl. Data Tables* **54** 1
[2] Palik E D (ed) 1985 *Handbook of Optical Constants of Solid* (Orlando, FL: Academic)
[3] Windt D L, Cash W C Jr, Scott M, Arendt P, Newnam B, Fisher R F and Swartzlander A B 1988 *Appl. Opt.* **27** 279
[4] Toll J S 1956 *Phys. Rev.* **104** 1760
[5] Hagemann H J, Clucher R and Nielson U 1973 *Prepint DESY* 41-73/10 pp 1–48
[6] Stern F 1963 *Solid State Physics* vol 15, ed F Seitz and D Turnbull (London: Academic)
[7] Young R H 1977 *J. Opt. Soc. Am.* **67** 520
[8] Plaskett J 1963 *J. Chem. Phys.* **38** 612
[9] Sinha S K, Sirota E B, Garoff S, Stanley H B 1988 *Phys. Rev.* B **38** 2297
[10] Birken H G, Kunz C, Wolf R 1990 *Phys. Scr.* **41** 385
[11] Borisova S S, Mikhailov I F, Kozhevnikov I V, Vinogradov A V 1991 *Opt. Acoust. Rev.* **1** 183
[12] Vinogradov A V, Zorev N N, Kozhevnikov I V, Sagitov S I and Turyanskii A G 1988 *Sov. Phys.–JETP* **94(9)** 203
[13] André J-M, Maquet A and Barchewitz R 1982 *Phys. Rev.* B **25** 5671
[14] Filatova E O, Stepanov A P and Lukyanov V A 1996 *Opt. Spectrosc.* **81** 416
[15] Filatova E O, Lukyanov V, Blessing C and Friedrich J 1996 *J. Electron Spectrosc. Relat. Phenom.* **79** 63